Mon. Not. R. Astron. Soc. **000**, 000–000 (0000) Printed 1 February 2008 (MN LATEX style file v1.4)

Primordial feature at the scale of superclusters of galaxies

Mirt Gramann and Gert Hütsi
Tartu Observatory, Tõravere 61602, Estonia

1 February 2008

ABSTRACT
We investigate a spatially-flat cold dark matter model (with the matter density parameter $\Omega_m = 0.3$) with a primordial feature in the initial power spectrum. We assume that there is a bump in the power spectrum of density fluctuations at wavelengths $\lambda \sim 30 - 60h^{-1}$Mpc, which correspond to the scale of superclusters of galaxies. There are indications for such a feature in the power spectra derived from redshift surveys and also in the power spectra derived from peculiar velocities of galaxies. We study the mass function of clusters of galaxies, the power spectrum of the CMB temperature fluctuations, the rms bulk velocity and the rms peculiar velocity of clusters of galaxies. The baryon density is assumed to be consistent with the BBN value. We show that with an appropriately chosen feature in the power spectrum of density fluctuations at the scale of superclusters, the mass function of clusters, the CMB power spectrum, the rms bulk velocity and the rms peculiar velocity of clusters are in good agreement with the observed data.

Key words: galaxies: clusters: general – cosmology: theory – dark matter – large-scale structure of Universe – cosmic microwave background.

1 INTRODUCTION

The spatially-flat cold dark matter (CDM) model (matter density parameter $\Omega_m = 0.3$, flatness being restored by a contribution from a cosmological constant $\Omega_\Lambda = 0.7$) with a scale-invariant initial conditions has been a standard model in cosmology over last five years (see e.g. Ostriker & Steinhardt 1995). This model successfully explains many large- and small-scale structure observations including the mass function and the peculiar velocities of clusters of galaxies. The flat cosmological model with the matter density parameter $\Omega_m = 0.3$ is also consistent with the observations of Type Ia supernovae at redshift $z \sim 1$ (Perlmutter at al. 1999; Riess et al. 1998).

In this paper we investigate the CDM model with a primordial feature in the initial power spectrum of density fluctuations. Adams, Ross & Sarkar (1997) have noted that according to our current understanding of the unification of fundamental interactions, there should have been phase transitions associated with spontaneous symmetry breaking during the inflationary era. This may have resulted in the breaking of scale-invariance of the initial power spectrum. Chung et al. (2000) studied an alternative mechanism that can alter classical motion of the inflaton and produce features in the initial power spectrum. They showed that if the inflaton is coupled to a massive particle, resonant production of the particle during inflation modifies the evolution of the inflaton, and may leave an imprint in the initial power spectrum. The spectral features in the initial spectrum may also be generated if the inflaton evolves through a kink in its potential (Starobinsky 1992; Lesgourgues, Polarski & Starobinsky 1998; Gramann & Hütsi 2000).

A number of different non-scale invariant initial conditions have been recently used to analyze the cosmic microwave background (CMB) data (see e.g. Kanasawa et al. 2000; Barriga et al. 2000; Atrio-Barandela et al. 2000; Griffiths, Silk & Zaroubi 2000; Hannestad, Hansen & Villante 2000; Wang & Mathews 2000). Griffiths, Silk & Zaroubi (2000) and Hannestad, Hansen & Villante (2000) showed that the CMB data favour a bump-like feature in the power spectrum around a scale of $k = 0.004h\mathrm{Mpc}^{-1}$. Barriga et al. (2000) studied the step-like spectral feature in the range $k \sim (0.06-0.6)h\mathrm{Mpc}^{-1}$ and found that such a spectral break enables a good fit to both the APM and CMB data. Atrio-Barandela et al. (2000) investigated the temperature power spectrum in the CDM models, where the power spectrum of density fluctuations at $z \sim 10^3$ was in the form $P(k) \sim k^{-1.9}$ at wavenumbers $k > 0.05h\mathrm{Mpc}^{-1}$. This power spectrum of density fluctuations was derived by Einasto et al. (1999) by analyzing different observed power spectra of galaxies and clusters of galaxies. Atrio-Barandela et al. (2000) found that this form of the power spectrum of density fluctuations is consistent with the recent CMB data. However, in this paper we examine the mass function of clusters of galaxies in the same model and find that for $\Omega_m = 0.3$, the number density of clusters is significantly smaller than observed.

Suhhonenko & Gramann (1999, hereafter SG) studied properties of clusters of galaxies in two cosmological models

which rely on the observed power spectra of the distribution of galaxies. In the first model (hereafter model 1), the power spectrum of density fluctuations at $z \sim 10^3$ was in the form $P(k) \sim k^{-2}$ at wavenumbers $k > 0.05h\mathrm{Mpc}^{-1}$. In the second model (hereafter model 2), the power spectrum contained a feature (bump) at wavenumbers $k \sim 0.1 - 0.2h\mathrm{Mpc}^{-1}$ ($\lambda \sim 30 - 60h^{-1}\mathrm{Mpc}$), which correspond to the scale of superclusters (see e.g. Einasto et al. 1997). SG examined the mass function, peculiar velocities, the power spectrum and the correlation function of clusters in both models and found that in many aspects the power spectrum of density fluctuations in model 2 fits the observed data better than the simple power-law model 1. This study suggested that probably at wavenumbers $k \sim 0.05 - 0.2h\mathrm{Mpc}^{-1}$, the power spectrum of density fluctuations is not a featureless simple power law.

Fig. 1 shows the power spectrum of density fluctuations in the CDM model examined in this paper (see eq. (5) below). We assume that there is a feature (bump) in the power spectrum at wavenumbers $k = 0.1 - 0.2h^{-1}$ Mpc. The power spectrum in the CDM model with a scale-invariant initial power spectrum is also plotted. It is assumed that the density parameter $\Omega_m = 0.3$ and the normalized Hubble constant $h = 0.65$. For comparison, we show in Fig. 1 the observed power spectra derived from the distribution of galaxies in the APM, Stromlo-APM and Durham/UKST surveys (Baugh & Efstathiou 1993; Tadros & Efstathiou 1996; Hoyle et al. 1999). For the Stromlo-APM and Durham/UKST surveys, we present estimates for the flux-limited sample with $P(k) = 8000h^{-3}$ Mpc^3 in the weighting function (see Tadros & Efstathiou 1996; Hoyle et al. 1999 for details). There are indications for a similar bump in the power spectrum derived from the Stromlo-APM survey. On the other hand, there is no similar feature in the APM and Durham/UKST power spectrum. Hoyle et al. (1999) analyzed the power spectrum for different volume-limited and flux-limited samples drawn from the Durham/UKST redshift survey. There are indications for a similar bump in the power spectrum measured in a volume limited sample with $z_{max} = 0.08$ (see Hoyle et al. (1999) for details).

We also examined the power spectrum derived from the distribution of galaxies in the SSRS2+CfA2 redshift survey (da Costa et al. 1994). There is a feature in the SSRS2+CfA2 power spectrum at wavenumbers $k = 0.1 - 0.2h^{-1}$ Mpc. Silberman et al. (2001) studied the power spectrum of peculiar velocities of galaxies and found an indication for a wiggle in the power spectrum: an excess near $k \sim 0.05h$ Mpc^{-1} and a deficiency at $k \sim 0.1h$ Mpc^{-1}. This wiggle in the power spectrum is similar to the spectral feature studied in this paper. Most recently, there are indications for such a feature in the preliminary power spectrum derived from part of the 2dF redshift survey (Percival et al. 2001).

SG studied the power spectrum of clusters using N-body simulations and showed that the power spectrum of clusters in model 2 is in good agreement with the observed power spectrum of the APM clusters determined by Tadros, Efstathiou & Dalton (1998). SG investigated also the relation between the power spectrum of clusters and the power spectrum of matter fluctuations and found that in this model the relation between the cluster power spectrum and matter power spectrum is not linear at wavenumbers $k > 0.1h\mathrm{Mpc}^{-1}$ (see also Gramann & Suhhonenko 1999).

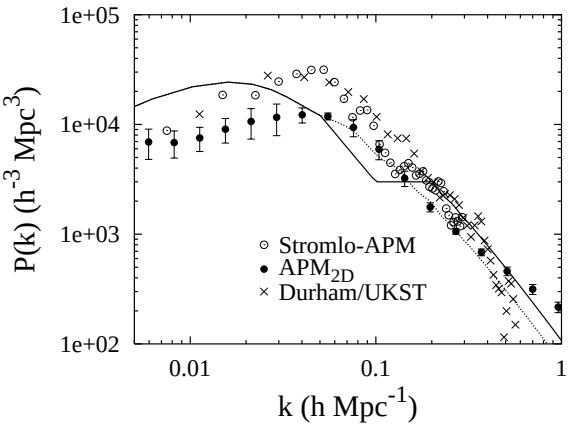

Figure 1. The power spectrum of density fluctuations in the CDM model examined in this paper (solid line) and in the standard CDM model with a scale-invariant initial power spectrum (dotted line). In the models studied, $\Omega_m = 0.3$ and $h = 0.65$. Filled circles, open circles and crosses show the power spectrum of the galaxy distribution in the APM, Stromlo-APM and Durham/UKST surveys, respectively. For clarity, error bars are only shown for the APM data.

In this paper we investigate the mass function of clusters of galaxies and the temperature power spectrum in the model with a bump in the power spectrum of density fluctuations at the scale of superclusters of galaxies. We also study the rms bulk velocity of galaxies and the rms peculiar velocity of clusters of galaxies in this model. The results are compared with observations. We examine the flat cosmological model with the density parameter $\Omega_m = 0.3$, the baryon density $\Omega_b h^2 = 0.019$ and the normalized Hubble constant $h = 0.65$ and $h = 0.70$. These values are in agreement with measurements of the density parameter (e.g. Bahcall et al. 1999), with measurements of the baryon density from abundances of light elements (O'Meara et al. 2001; Tytler et al. 2000) and with measurements of the Hubble constant using various distance indicators (Freedman et al. 2000; see also Parodi et al. 2000). The Hubble constant is given as $H_0 = 100h$ km s^{-1} Mpc^{-1}. To restore the spatial flatness in the low density model, we assume a contribution from a cosmological constant $\Omega_\Lambda = 0.7$.

To study the mass function of clusters we use the Press-Schechter (Press-Schechter 1974, hereafter PS) approximation. The transfer functions $T(k)$ and the temperature power spectra are calculated using the fast Boltzmann code CMBFAST developed by Seljak & Zaldarriaga (1996). The code CMBFAST has been modified to incorporate a primordial feature in the initial power spectrum. We assume that the initial fluctuations are adiabatic and that the initial density fluctuation field is a Gaussian field. In this case, the power spectrum provides a complete statistical description of the field.

This paper is organized as follows. In Section 2 we study the mass function of clusters of galaxies and temperature power spectrum in our model, and compare the results with observations. In Section 3 we examine peculiar velocities of galaxies and clusters of galaxies. Discussion and summary are presented in Section 4.

2 THE MASS FUNCTION OF CLUSTERS AND CMB ANISOTROPIES

Let us first consider the CDM model, where the power spectrum of density fluctuations at $z \sim 10^3$ is in the form

$$P(k) = AkS(k)T^2(k) = \begin{cases} AkT^2(k), & \text{if } k < k_0; \\ P(k_0)(k/k_0)^{-1.9}, & \text{if } k > k_0, \end{cases} \quad (1)$$

where $k_0 = 0.05h$ Mpc^{-1}. Here, the initial power spectrum is defined as $P_{in}(k) = AkS(k)$ and $T(k)$ is the transfer function, which describes the modification of the initial power spectrum during the era of radiation domination. The function $S(k)$ describes the deviation of the initial power spectrum from a scale invariant form $P(k) \sim k$. The normalization constant A is determined by the large-scale CMB anisotropy. This form of the power spectrum at wavenumbers $k > 0.05h$Mpc^{-1} was derived by Einasto et al. (1999) by analyzing different observed power spectra of galaxies and clusters of galaxies. We denote the CDM model, were the power spectrum is in the form (1), as model 1.

Fig. 2a shows the power spectrum of density fluctuations in model 1 for $h = 0.65$ and $h = 0.70$. We also show the power spectrum in the CDM model with a scale-invariant spectrum ($S(k) \equiv 1$). In comparison with the standard model, the power spectrum of density fluctuations in model 1 is depressed at wavenumbers $k > 0.05h$Mpc^{-1}. A similar break in the power spectrum of density fluctuations was analyzed by Atrio-Barandela et al. (2000).

To calculate the angular power spectrum of the CMB temperature fluctuations, we used the code CMBFAST, which was modified to incorporate the function $S(k)$ in the initial power spectrum. We examined the models with no reionization (optical depth $\tau = 0$). Fig. 2b shows the CMB power spectrum, $\Delta T_l^2 = l(l+1)C_l/2\pi$, predicted in model 1. Here $C_l = \langle a_{lm}^2 \rangle$ and a_{lm} are the coefficients of the spherical harmonic decomposition of the CMB temperature field: $\Delta T(\theta, \varphi) = \sum a_{lm} Y_{lm}(\theta, \varphi)$. Fig. 2b shows also the temperature power spectrum predicted in the standard CDM model. We see that lowering the amplitude of the power spectrum at wavenumbers $k > 0.05h^{-1}$Mpc, lowers also the amplitude of the temperature power spectrum at multipoles $l > 400$. The height of the first peak is different in the models in Fig. 2b due to the change in Hubble's constant.

Fig. 2b shows also the CMB power spectrum derived from the Boomerang (Netterfield et al. 2001) and from the Maxima-1 (Hanany et al. 2000) experiments. We see that the temperature power spectrum in model 1 is consistent with the observed temperature power spectrum. The amplitude of the second acoustic peak at $l \sim 500$ in the observed temperature power spectrum is smaller than that predicted in the standard CDM model with $\Omega_m = 0.3$. However, in the analyzes we have assumed that the spectral index $n = 1$ and the optical depth $\tau = 0$. Also, both CMB datasets have a calibration uncertainty and a beam uncertainty that are not included in the errors plotted in Fig. 2b. Netterfield et al. (2001) analyzed the CMB power spectrum in the standard CDM model in more detail and showed that this model is consistent with the observed CMB data, once the parameters $n \neq 1$ and $\tau \neq 0$, and beam and calibration uncertainties are taken into account.

To study the mass function of clusters we use the Press-Schechter (1974, PS) approximation. The PS mass function has been compared with N-body simulations (Efstathiou et al. 1988; White, Efstathiou & Frenk 1993; Lacey & Cole 1994; Eke, Cole & Frenk 1996) and has been shown to provide an accurate description of the abundance of virialized cluster-size halos. In the PS approximation the number density of clusters with the mass between M and $M + dM$ is

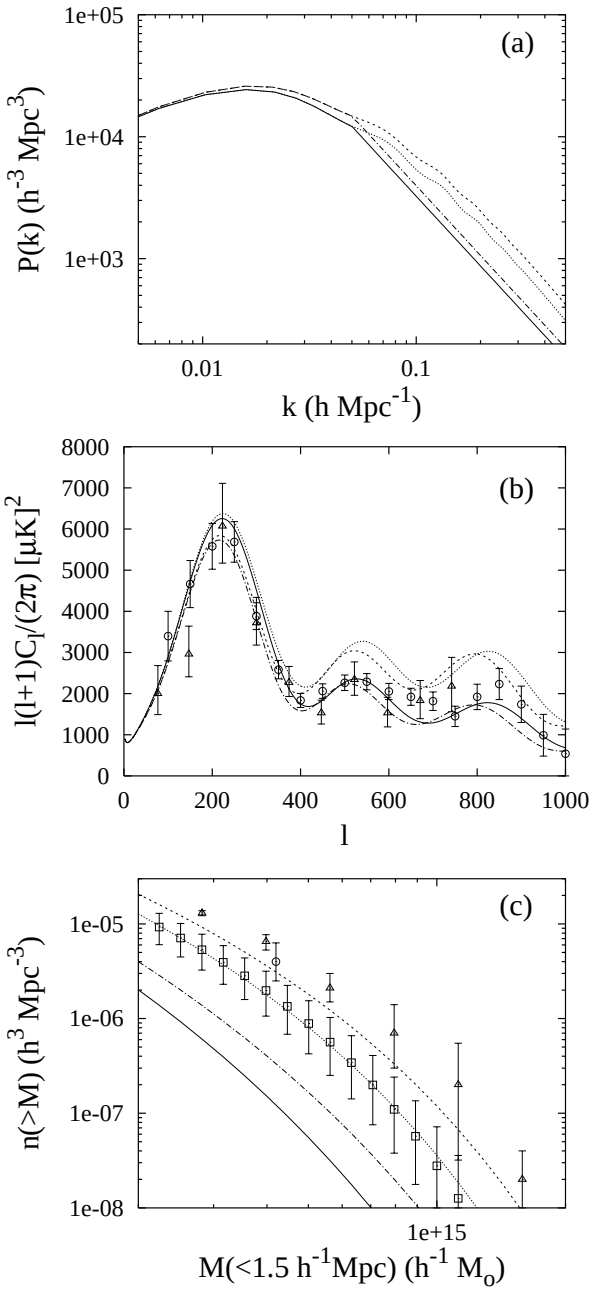

Figure 2. (a) The power spectrum of density fluctuations in model 1 for $h = 0.65$ (solid line) and for $h = 0.70$ (dot-dashed line). The dotted line and dashed line show the power spectrum in the standard CDM model for $h = 0.65$ and $h = 0.70$, respectively. (b) CMB power spectrum in the same models. The data are from the Boomerang (circles) and Maxima-1 (triangles) experiments. (c) The cluster mass function in the same models. Squares and triangles show the cluster mass function derived by Bahcall & Cen (1993) and Girardi et al. (1998), respectively. The circle represents the result obtained by White et al. (1993)

given by

$$n(M)dM = -\sqrt{\frac{2}{\pi}}\frac{\rho_b}{M}\frac{\delta_t}{\sigma^2(M)}\frac{d\sigma(M)}{dM}\exp\left[-\frac{\delta_t^2}{2\sigma^2(M)}\right]dM. \quad (2)$$

Here ρ_b is the mean background density and δ_t is the linear theory overdensity for a uniform spherical fluctuation which is now collapsing; $\delta_t = 1.675$ for $\Omega_0 = 0.3$ (Eke et al. 1996). The function $\sigma(M)$ is the rms linear density fluctuation at the mass scale M. We will use the top-hat window function to describe halos. For the top-hat window, the mass M is related to the window radius R as $M = 4\pi\rho_b R^3/3$. In this case, the number density of clusters of mass larger than M can be expressed as

$$n_{cl}(>M) = \int_M^\infty n(M')dM' =$$

$$= -\frac{3}{(2\pi)^{3/2}}\int_R^\infty \frac{\delta_t}{\sigma^2(r)}\frac{d\sigma(r)}{dr}\exp\left[-\frac{\delta_t^2}{2\sigma^2(r)}\right]\frac{dr}{r^3}. \quad (3)$$

Fig. 2c shows the cluster mass function predicted in model 1 for $h = 0.65$ and $h = 0.70$. The mass function in the standard CDM model is also plotted. We investigated the cluster masses within a $1.5h^{-1}$ Mpc radius sphere around the cluster center. This mass $M_{1.5}$ is related to the window radius R as

$$R = 8.43\Omega_0^{\frac{0.2\alpha}{3-\alpha}}\left[\frac{M_{1.5}}{6.99\times10^{14}\Omega_0 h^{-1}M_\odot}\right]^{\frac{1}{3-\alpha}}(h^{-1}\mathrm{Mpc}). \quad (4)$$

Here the parameter α describes the cluster mass profile, $M(r) \sim r^\alpha$, at radii $r \sim 1.5h^{-1}$ Mpc. Numerical simulations and observations of clusters indicate that the parameter $\alpha \approx 0.6 - 0.7$ for most of clusters (e.g. Navarro, Frenk & White 1995; Carlberg, Yee & Ellingson 1997). In this paper we use the value $\alpha = 0.65$.

Fig. 2c also shows the mass function of clusters derived by Bahcall & Cen (1993, hereafter BC) and by Girardi et al. (1998, hereafter G98). BC used both optical and X-ray observed properties of clusters to determine the mass function of clusters. The function was extended towards the faint end using small groups of galaxies. G98 determined the mass function of clusters by using virial mass estimates for 152 nearby Abell-ACO clusters including the ENACS data (Katgert et al. 1998). The mass function derived by G98 is somewhat larger than the mass function derived by BC, the difference being larger at larger masses (see Fig. 2c). Reiprich & Bohringer (1999) determined the cluster mass function using X-ray flux-limited sample from ROSAT All-Sky survey. They determined the masses for different outer radii of the clusters and for a radius $r = 1.5h^{-1}$ Mpc their mass function agrees with that determined by BC.

Let us consider the amplitude of the mass function of galaxy clusters at $M_{1.5} = 4\cdot10^{14}h^{-1}M_\odot$. For this mass, the cluster abundances derived by BC and G98 are $n(>M) = (2.0\pm1.1)\cdot10^{-6}h^3\mathrm{Mpc}^{-3}$ and $n(>M) = (6.3\pm1.2)\cdot10^{-6}h^3\mathrm{Mpc}^{-3}$, respectively. By analysing X-ray properties of clusters, White, Efstathiou & Frenk (1993) found that the number density of clusters with the mass $M_{1.5} \approx 4.2\cdot10^{14}h^{-1}M_\odot$ is $n(>M) = 4\cdot10^{-6}h^3\mathrm{Mpc}^{-3}$.

Fig. 2c shows that the cluster mass function in the standard CDM model is in good agreement with the observed data. But the number density of clusters in model 1 is substantially lower than observed; for the mass $M_{1.5} = 4\cdot10^{14}h^{-1}M_\odot$, the cluster abundance $n(>M) = 1.5\cdot10^{-7}h^3\mathrm{Mpc}^{-3}$ and $n(>M) = 4.1\cdot10^{-7}h^3\mathrm{Mpc}^{-3}$ for $h = 0.65$ and $h = 0.70$, respectively.

In model 1, the amplitude of the power spectrum of density fluctuations is depressed with respect to the standard CDM model for $k > 0.05h\mathrm{Mpc}^{-1}$. Lowering the amplitude of the power spectrum of density fluctuations at wavenumbers $k > 0.05h$ Mpc^{-1} lowers also the CMB power spectrum at multipoles $l > 400$. However, lowering the amplitude of the power spectrum of density fluctuations lowers also the cluster mass function, and as a result in model 1 the number density of clusters is smaller than observed. One possibility to get rid of the last effect is to consider a bump in the power spectrum of density fluctuations at wavenumbers $k \sim 0.1 - 0.2h^{-1}$Mpc. The cluster mass function for masses $M \sim 10^{14} - 10^{15}h^{-1}M_\odot$ is sensitive to the amplitude of the power spectrum at wavenumbers $k \sim 0.2h^{-1}$Mpc, while the temperature anisotropy at the second acoustic peak is sensitive to the amplitude of the power spectrum at wavenumbers $k \sim 0.05 - 0.1h^{-1}$Mpc.

Thus let us now study a CDM model, where the power spectrum of density fluctuations at $z \sim 10^3$ contains a specific feature at wavenumbers $k \sim 0.1 - 0.2h\mathrm{Mpc}^{-1}$ ($\lambda \sim 30 - 60h^{-1}$Mpc) which correspond to the scale of superclusters:

$$P(k) = AkS(k)T^2(k) = \begin{cases} AkT^2(k), & \text{if } k < k_0; \\ P(k_0)(k/k_0)^m, & \text{if } k_0 < k < k_1; \\ P(k_1), & \text{if } k_1 < k < k_2; \\ BkT^2(k), & \text{if } k > k_2, \end{cases} \quad (5)$$

where $k_0 = 0.05h\mathrm{Mpc}^{-1}$, the spectral index $m = \log[P(k_1)/P(k_0)]/\log[k_1/k_0]$ and $B = P(k_1)/(k_2T^2(k_2))$. This form of the power spectrum contains three free parameters, which describe the bump in the power spectrum: k_1, k_2 and $P(k_1)$. The parameter k_1 determines the beginning of the bump, the parameter k_2 - the end of the bump, and the parameter $P(k_1)$ - the amplitude of the power spectrum for the bump. In this paper we examine the models where $k_1 = 0.1h\mathrm{Mpc}^{-1}$, $k_2 = 0.2h\mathrm{Mpc}^{-1}$ and $P(k_1) = 2500 - 3500h^{-3}\mathrm{Mpc}^3$. We denote the CDM model, where the power spectrum is in the form (5), as model 2.

Fig. 3a shows the power spectrum of density fluctuations in model 2 for different values of the parameter $P(k_1)$. In the models studied, $P(k_1) = 2500, 3000$ and $3500h^{-3}\mathrm{Mpc}^3$. The normalized Hubble constant $h = 0.65$. In Fig. 3b, we show the function $S(k)$, which describes the deviation of the initial power spectrum from the scale-invariant form. The function $S(k) = 1$ at wavenumbers $k < 0.05h\mathrm{Mpc}^{-1}$, reaches the minimum at $k_1 = 0.1h\mathrm{Mpc}^{-1}$ and then increases up to the wavenumber $k_2 = 0.2h\mathrm{Mpc}^{-1}$. At the minimum, $S(k_1) = 0.48$ and $S(k_1) = 0.67$ for $P(k_1) = 2500h^{-3}$ Mpc^3 and $P(k_1) = 3500h^{-3}\mathrm{Mpc}^3$, respectively. For wavenumbers $k > 0.2h\mathrm{Mpc}^{-1}$, we find that $S(k) = 1.3$ and $S(k) = 1.9$, respectively. We investigated also the CDM model with $h = 0.70$ assuming that $P(k_1) = 2500, 3000$ and $3500h^{-3}$ Mpc^3. In this model, $S(k_1) = 0.38$, $S(k_2) = 1.0$ and $S(k_1) = 0.52$, $S(k_2) = 1.4$ for the parameter $P(k_1) = 2500h^{-3}$ Mpc^3 and $P(k_1) = 3500h^{-3}\mathrm{Mpc}^3$, respectively.

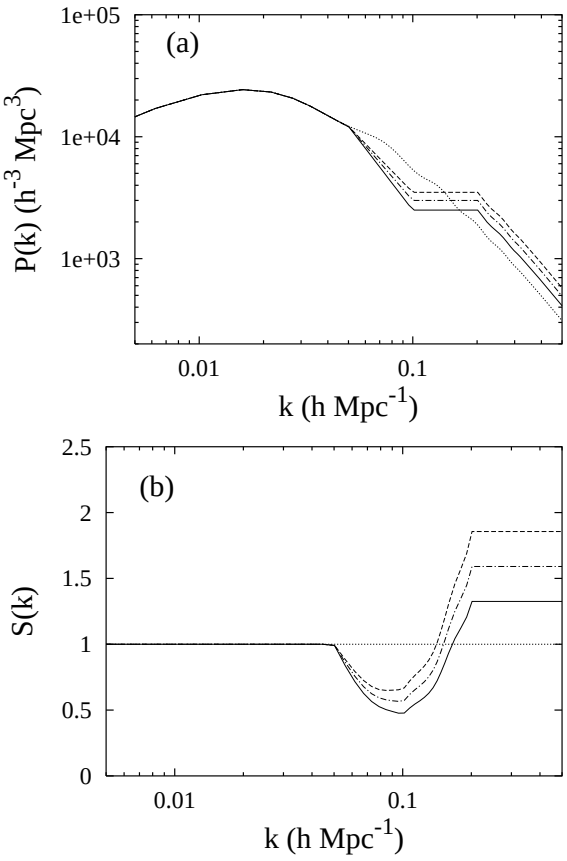

Figure 3. (a) The power spectrum of density fluctuations in model 2 for $P(k_1) = 2500h^{-3}\mathrm{Mpc}^3$ (solid line), for $P(k_1) = 3000h^{-3}\mathrm{Mpc}^3$ (dot-dashed line) and for $P(k_1) = 3500h^{-3}\mathrm{Mpc}^3$ (dashed line). The dotted line shows the power spectrum in the standard CDM model. (Here $h = 0.65$.) (b) The function $S(k)$ in the same models as in the panel (a).

Fig. 4 shows the variance, $\sigma^2(R)$, in the standard CDM model and in model 2 for different values of the parameter $P(k_1)$. The variance is given as a function of top-hat window radius R. For the masses $M_{1.5} = 10^{14}h^{-1}M_\odot$ and $M_{1.5} = 10^{15}h^{-1}M_\odot$, the window radius $R = 5.8h^{-1}$ Mpc and $R = 15.3h^{-1}$ Mpc, respectively (see eq. (4)).

Fig. 5 shows the cluster mass function as predicted in model 2 for the parameter $P(k_1) = 2500, 3000$ and $3500h^{-3}$ Mpc^3. The mass function of clusters in the standard CDM model is also plotted. Fig. 5a shows the results for $h = 0.65$ and Fig. 5b for $h = 0.70$. In model 2, the mass function is steeper than that in the standard CDM model. At the same value of $P(k_1)$, the cluster mass function for $h = 0.65$ and $h = 0.70$ is similar. For comparison, we also show in Fig.5 the observed mass function of clusters of galaxies derived by BC and G98. In the models studied, the cluster mass function is consistent with the observed data. If $h = 0.65$, then for the mass $M_{1.5} = 4 \cdot 10^{14}h^{-1}M_\odot$, the cluster abundance $n(> M) = 1.4 \cdot 10^{-6}h^3\mathrm{Mpc}^{-3}$ and $n(> M) = 3.5 \cdot 10^{-6}h^3\mathrm{Mpc}^{-3}$ for $P(k_1) = 2500h^{-3}\mathrm{Mpc}^3$ and $P(k_1) = 3500h^{-3}$ Mpc^3, respectively. (If $h = 0.70$, $n(> M) = 1.5 \cdot 10^{-6}h^3\mathrm{Mpc}^{-3}$ and $n(> M) = 3.7 \cdot 10^{-6}h^3\mathrm{Mpc}^{-3}$, respectively.)

Fig. 6 demonstrates the angular power spectrum of the CMB temperature fluctuations as predicted in model 2. We also show the temperature power spectrum in the standard CDM model with a scale-invariant power spectrum. Fig. 6a demonstrates the results for $h = 0.65$ and Fig. 6b for $h = 0.70$. In model 2, the amplitude of the temperature power spectrum at multipoles $l > 400$ is smaller than that predicted in the standard CDM model. Fig. 6 also shows the CMB power spectrum derived from the Boomerang (Net-

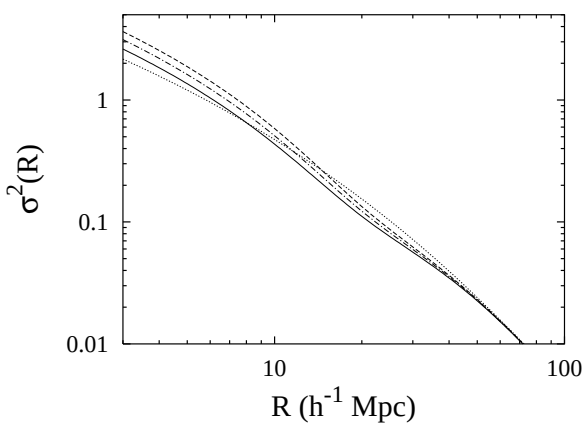

Figure 4. The variance $\sigma^2(R)$ in the same models as in Fig. 3, shown with the same line types.

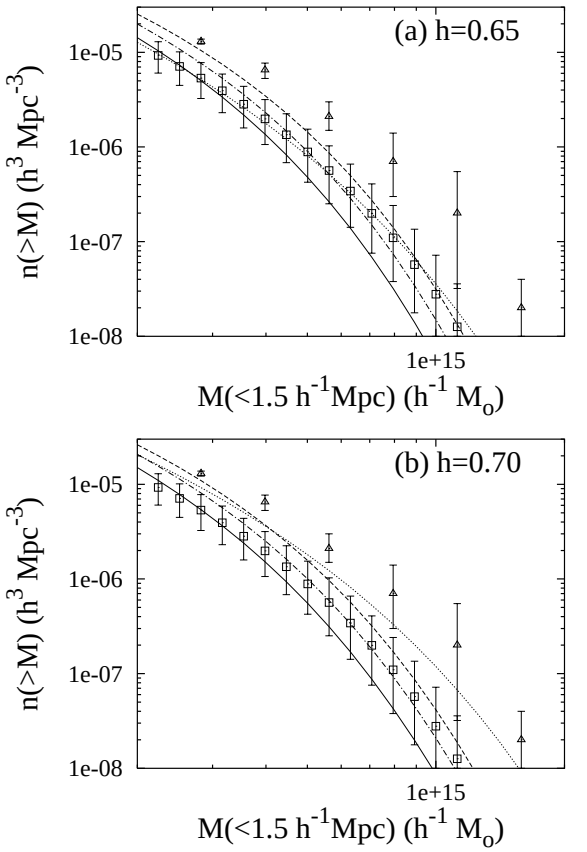

Figure 5. The mass function of clusters as predicted in model 2. (a) h=0.65. (b) h=0.70. The lines are specified similarly to the Fig. 3. Squares and triangles show the mass function of galaxy clusters derived by Bahcall & Cen (1993) and Girardi et al. (1998), respectively.

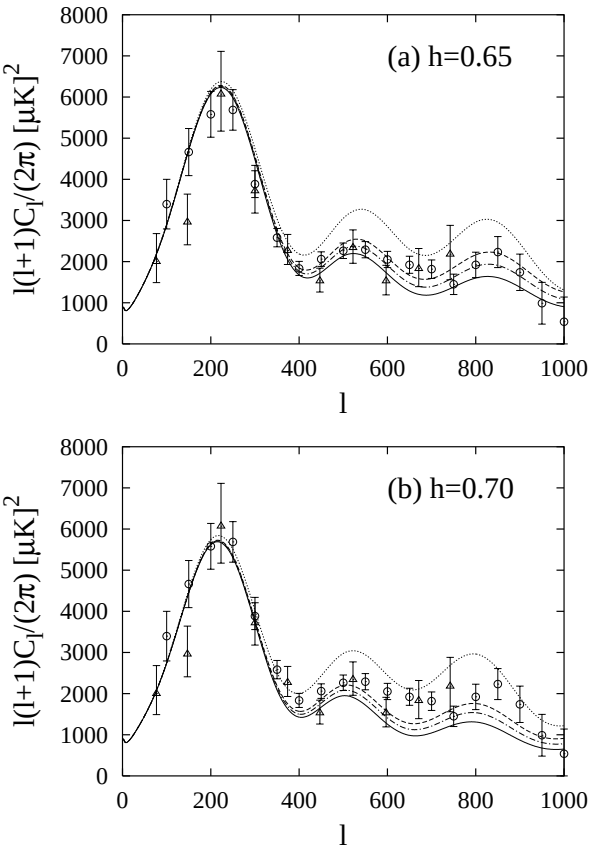

Figure 6. The power spectrum of the CMB temperature in the same models as in Fig. 3, shown with the same line types. (a) h=0.65. (b) h=0.70. The observational data are from the Boomerang (circles) and Maxima-1 (triangles) experiments.

terfield et al. 2001) and from the Maxima-1 (Hanany et al. 2000) experiments. In the models studied, the temperature power spectrum is consistent with the observed temperature power spectrum.

Therefore, in the model with a bump in the power spectrum of density fluctuations at the scale of superclusters, the mass function of clusters and the temperature power spectrum are in good agreement with the observed data.

3 PECULIAR VELOCITIES

The observed rms peculiar velocity of galaxy clusters has been studied in several papers (e.g. Bahcall, Gramann & Cen 1994, Bahcall & Oh 1996, Borgani et al. 1997, Watkins 1997, Dale et al. 1999). Watkins (1997) developed a likelihood method for estimating the rms peculiar velocity of clusters from line-of-sight velocity measurements and their associated errors. This method was applied to two observed samples of cluster peculiar velocities: a sample known as the SCI sample (Giovanelli et al. 1997) and a subsample of the Mark III catalog (Willick et al. 1997). Watkins (1997) found that the rms one-dimensional cluster peculiar velocity is 265^{+106}_{-75} km s^{-1}, which corresponds to the three-dimensional rms velocity 459^{+184}_{-130} km s^{-1}. Dale et al. (1999) obtained Tully-Fisher peculiar velocities for 52 Abell clusters distributed throughout the sky between ~ 50 and $200h^{-1}$Mpc.

Table 1. Peculiar velocities in the different models.

h	$P(k_1)$ (h^{-3}Mpc^{-3})	v_{cl} (km s^{-1})	V_{60} (km s^{-1})
0.65	2500	557	273
	3000	578	273
	3500	598	273
0.70	2500	579	284
	3000	599	284
	3500	619	284

They found that the rms one-dimensional cluster peculiar velocity is 341 ± 93km s^{-1}, which corresponds to the three-dimensional rms velocity 591 ± 161 km s^{-1}.

To investigate peculiar velocities of clusters in our models, we use the linear theory predictions for peculiar velocities of peaks in the Gaussian field. The linear rms velocity fluctuation on a given scale R at the present epoch can be expressed as

$$\sigma_v(R) = H_0 f(\Omega_0)\sigma_{-1}(R), \tag{6}$$

where $f(\Omega_0) \approx \Omega_0^{0.56}$ is the linear velocity growth factor in the flat models and σ_j is defined for any integer j by

$$\sigma_j^2 = \frac{1}{2\pi^2}\int P(k)W^2(kR)k^{2j+2}dk. \tag{7}$$

Bardeen et al. (1986) showed that the rms peculiar velocity at peaks of the smoothed density field differs systematically from $\sigma_v(R)$, and can be expressed as

$$\sigma_p(R) = \sigma_v(R)\sqrt{1-\sigma_0^4/\sigma_1^2\sigma_{-1}^2}. \tag{8}$$

SG examined the linear theory predictions for the peculiar velocities of peaks and compared these to the peculiar velocities of clusters in N-body simulations. The N-body clusters were determined as peaks of the density field smoothed on the scale $R \sim 1.5h^{-1}$ Mpc. The numerical results showed that the rms peculiar velocity of small clusters is similar to the linear theory expectations, while the rms peculiar velocity of rich clusters is higher than that predicted in the linear theory. The rms peculiar velocity of clusters with a mean cluster separation $d_{cl} = 30h^{-1}$ Mpc was ~ 18 per cent higher than that predicted by the linear theory. We assume that the observed cluster samples studied by Watkins (1997) and Dale et al. (1999) correspond to the model clusters with a separation $d_{cl} \sim 30h^{-1}$ Mpc ($n_{cl} \sim 3.7 \cdot 10^{-5}h^3$ Mpc^{-3}) and determine the rms peculiar velocity of the clusters, v_{cl}, as

$$v_{cl} = 1.18\,\sigma_p(R), \tag{9}$$

where the radius $R = 1.5h^{-1}$ Mpc.

In the standard CDM model with $\Omega_m = 0.3$, we found that $v_{cl} = 582$ km s^{-1} and $v_{cl} = 635$ km s^{-1} for $h = 0.65$ and $h = 0.70$, respectively. Table 1 lists the rms peculiar velocity of clusters, v_{cl}, in our models. The rms peculiar velocity of clusters is $\sim 555 - 620$ km s^{-1}, which is consistent with the observed rms peculiar velocity of clusters derived by Watkins (1997) and Dale et al. (1999).

We also studied the rms bulk velocity for a radius $r = 60h^{-1}$Mpc, V_{60}. The rms bulk velocity was determined by using equation (6). In the standard $\Omega_m = 0.3$ model, $V_{60} = 273$ km s^{-1} and $V_{60} = 285$ km s^{-1} for $h = 0.65$ and $h =$

0.70, respectively. Table 1 lists the rms bulk velocity, V_{60}, in our models. The bulk velocity is similar to that in the standard model. The observed bulk velocities are determined in a sphere centred on the Local Group and represent a single measurement of the bulk flow on large scales. The observed bulk velocity derived from the Mark III catalogue of peculiar velocities for $r = 60h^{-1}$ Mpc is 370 ± 110 km s^{-1} (Kolatt & Dekel 1997). Giovanelli et al. (1998) studied the bulk velocity in the SCI sample and estimated that the bulk flow of a sphere of radius $r = 60h^{-1}$ Mpc is between 140 and 320 km s^{-1}. In the models studied, the rms bulk velocity is $\sim 275 - 285$ km s^{-1}, which is consistent with the observed data.

4 DISCUSSION AND SUMMARY

In this paper we have examined a CDM model, where the power spectrum contains a specific feature (bump) at the wavenumbers $k \sim 0.1{-}0.2h^{-1}$ Mpc, which correspond to the scale of superclusters of galaxies. We studied a flat cosmological model with the density parameter $\Omega_m = 0.3$ and the normalized Hubble constant $h = 0.65$ and $h = 0.70$. The baryon density was assumed to be consistent with the standard big-bang nucleosynthesis (BBN) value. We investigated the mass function of clusters and the angular power spectrum of the CMB temperature fluctuations, assuming different values of the spectral parameter $P(k_1)$ that determines the amplitude of the power spectrum for the bump. We found that the cluster mass function and the CMB power spectrum are in good agreement with the observed data if the spectral parameter $P(k_1)$ is in the range $P(k_1) = 2500 - 3500h^{-3}$Mpc^3. We also investigated the rms peculiar velocity of clusters and the rms bulk velocity for a radius $r = 60h^{-1}$ Mpc. In the models studied, the rms peculiar velocity of clusters is $\sim 555 - 620$ km s^{-1} and the rms bulk velocity is $\sim 275 - 285$ km s^{-1}, which are consistent with the observed data.

Therefore, in many aspects the CDM model, where the power spectrum contains a feature at the scale of superclusters of galaxies, fits the observed data. This model predicts that there is a bump in the correlation function of clusters at separations $r \sim 20 - 35h^{-1}$Mpc (Suhhonenko & Gramann 1999). In the future, accurate measurements of the cluster correlation function at these distances can serve as a discriminating test for this model.

What could be the origin of the primordial feature examined in this paper (see Fig. 3b)? The standard inflationary prediction concerning the initial power spectrum of density fluctuations is a simple power law: $P_{in} \sim k^n$. However, for more than ten years, there has been some interest in models called broken-scale-invariant (BSI), predicting deviations from a power-law. These models generally involve, in addition to the usual inflation field, other (effective) fields, driving successive stages of inflation or just triggering a phase transition (e.g. Starobinsky 1985; Kofman, Linde & Starobinsky 1985; Kofman & Pogosyan 1988; Gottlöber, Müller & Starobinsky 1991). Recently, there have been efforts to implement double/multiple inflation in realistic supersymmetric contexts (Lesgourgues 1998). There has also been an attempt to generate spectral features via resonant production of particles during inflation (Chung et al. 2000). Clearly, further work is needed to explain the primordial feature introduced in this paper in the context of different inflationary models.

ACKNOWLEDGEMENTS

We thank J. Einasto, M. Einasto and E. Saar for useful discussions. This work has been supported by the ESF grant 3601.

REFERENCES

Adams J.A., Ross G.G., Sarkar S., 1997, Nucl. Phys., B503, 405
Atrio-Barandela F., Einasto J., Müller V., Mücket J. P., Starobinsky A.A., 2000, preprint (astro-ph: 0012320)
Bahcall N.A., Cen R., 1993, ApJ, 407, L49 (BC)
Bahcall N.A., Oh S.P. 1996, ApJ, 462, L49
Bahcall N.A., Gramann M., Cen R. 1994, ApJ, 436, 23
Bahcall N.A., Ostriker J.P., Perlmutter S., Steinhardt P.J. 1999, Science, 1481
Bardeen J.M., Bond J.R., Kaiser N., Szalay A.S. 1986, ApJ, 304, 15
Barriga J., Gaztanaga E., Santos M.G., Sarkar S., 2000, MNRAS, in press (astro-ph: 0011398)
Baugh C., Efstathiou G., 1993, MNRAS, 265, 145
Borgani S., Da Costa L.N., Freudling W., Giovanelli R., Haynes M.P., Salzer J., Wegner G., 1997, ApJ, 482, L121
Carlberg R.G., Yee H.K.C., Ellingson E. 1997, ApJ, 479, L19
Chung D.J.J., Kolb E.W., Riotto A., Tkachev I.I., 2000, Phys. Rev., D62, 043508
da Costa L.N., Vogeley M.S., Geller M.J., Huchra J.P., Park C., 1994, ApJ, 437, L1
Dale D. A., Giovanelli R., Haynes M.P., Campusano L. E., Hardy E., 1999, AJ, 118, 1489
Einasto J. et al., 1999, ApJ, 519, 441
Einasto M., Tago E., Jaaniste J., Einasto J., Andernach H., 1997, A&AS, 123, 119
Efstathiou G., Frenk C.S., White S.D.M., Davis M. 1988, MNRAS, 235, 715
Eke V. R., Cole S., Frenk C. S. 1996, MNRAS, 282, 263
Freedman W.L. et al., 2000, ApJ, in press (astro-ph: 0012376)
Girardi M., Borgani S., Giuricin G., Mardirossian F., Mezetti M. 1998, ApJ, 506, 45 (G98)
Giovanelli R., Haynes M.P., Herter T., Vogt N.P., Wegner G., Salzer J.J., da Costa L.N., Freudling W., 1997, AJ, 113, 22
Giovanelli R., Haynes M.P., Salzer J.J., Wegner G., da Costa L.N., Freudling W., 1998, AJ, 116, 2632
Gottlöber S.,Müller V., Starobinsky A.A., 1991, Phys. Rev., D43, 2510
Gramann M., Hütsi G., 2000, MNRAS, 316, 631
Gramann M., Suhhonenko I., 1999, ApJ, 519, 433
Griffiths L. M., Silk J., Zaroubi S., 2000, preprint (astro-ph: 0010571)
Hanany S. et al. (Maxima collab.), 2000, ApJ, 545, L5
Hannestad S., Hansen S.H., Villante F.L., 2000, preprint (astro-ph: 0012009)
Hoyle F., Baugh C.M., Shanks T., Ratcliffe A., 1999, MNRAS, 309, 659
Kanazawa T., Kawasaki M., Sugiyama N., Yanagida T., 2000, Phys. Rev. D., 61, 023517
Katgert P., Mazure A., den Hartog R., Adami C., Biviano A., Perea J., 1998, A & AS, 129, 399
Kolatt T., Dekel A., 1997, ApJ, 479, 592
Kofman L.A., Linde A.D., Starobinsky A.A., 1985, Phys. Lett., B157, 361
Kofman L.A., Pogosyan D., 1988, Phys. Lett., B214, 508

Lacey C., Cole S. 1994, MNRAS, 271, 676
Lesgourgues J., 1998, Phys. Lett., B452, 15
Lesgourgues J., Polarski D., Starobinsky A. A., 1998, MNRAS, 297, 769
O'Meara J.M., Tytler D., Kirkman D., Suzuki N., Prochaska J.X., Lubin D., Wolfe A.M., 2001, ApJ in press (May 10 issue) (astro-ph: 0011179)
Navarro J.F., Frenk C.S, White S.D.M. 1996, ApJ, 462, 563
Netterfield C.B. et al. (Boomerang collab.), 2001, preprint (astro-ph: 0104460)
Ostriker J.P.,Steinhardt P.J., 1995, Nature, 377, 600
Parodi B.R., Saha A., Tammann G.A., Sandage A., 2000, ApJ, 540, 634
Peebles P.J.E, Seager S., Hu W., 2000, ApJ, 539, L1
Percival W.J. et al. (2dF collaboration), 2001, in preparation
Perlmutter S. et al., 1999, ApJ, 517, 565
Press W.H., Schechter P. 1974, ApJ, 187, 425
Reiprich T. H., Böhringer H., 1999, in Abstracts of the 19th Texas Symposium on Relativistic Astrophysics and Cosmology. Eds: J. Paul, T. Montmerle, and E. Aubourg, Paris. (astro-ph: 9908357)
Riess A.G. et al., 1998, AJ, 116, 1009
Seljak U., Zaldarriaga M., 1996, ApJ, 469, 7
Silberman L., Dekel A., Eldar A., Zehavi I., 2001, ApJ submitted (astro-ph: 0101361)
Starobinsky A.A., 1985, JETP Lett., 42, 152
Suhhonenko I., Gramann M., 1999, MNRAS, 303, 77 (SG)
Sutherland W. et al., 1999, MNRAS, 308, 289
Tadros H., Efstathiou G., 1996, MNRAS, 282, 1381
Tadros H., Efstathiou G., Dalton G.B., 1998, MNRAS, 262, 1023
Tegmark M., Zaldarriaga M., 2000, Phys. Rev. Lett., 85, 2240
Tytler D., O'Meara J.M., Suzuki N., Lubin, D. 2000, Phys. Scr., 85, 12
Wang Y., Mathews G., 2000, preprint (astro-ph:0011351)
Watkins R. 1997, MNRAS, 292, L59
White S.D.M., Efstathiou G., & Frenk C.S. 1993, MNRAS, 262, 1023
Willick J.A., Courteau S., Faber S. M., Burstein D., Dekel A., Strauss M. A., 1997, ApJS, 109, 333